Journal of Computational Applied Mechanics 2026, 57(1): 63-83

DOI: 10.22059/jcamech.2025.403627.1630

RESEARCH PAPER

A Caputo Time-Fractional Derivative Approach to Pulsatile Non-Newtonian Sutterby Blood Fluid Flow through a Vertical Stenotic Artery under MHD Influence

M. H. Shah [a], R. Ellahi [b,*] , A. Zeeshan [b,c], T. Abbas [d]

[a] *Department of Geological Sciences, University of Alabama, Tuscaloosa, AL, USA*
[b] *Department of Mathematics & Statistics, International Islamic University, Islamabad, Pakistan*
[c] *Department of Mathematics, College of Science, Korea University, 145 Anam-ro, Seongbuk-gu, Seoul 02841, Republic of Korea*
[d] *Departrment of Mathematics, Division of Science and Technology, University of Education, Lahore, Pakistan*

Abstract

Blood flow through arteries is essential for maintaining metabolism of the body. Tissue injury and metabolic issues can develop from a deficiency of blood supply. A stenotic artery can be a major cause of this deficiency of blood supply. It is interesting to note that new studies have shown that magnetic fields can benefit different body parts, including the cardiovascular system. In this study, blood is considered Sutterby fluid with time fractional derivative, to examine effect of a magnetic field as well as fractional parameter on blood flow past a stenotic artery. In addition, the thermal behavior of the flow due to electromagnetic interactions and radiative heat flux is considered. We obtained numerical solutions of coupled nonlinear momentum and energy equations by using finite difference method. A thorough graphical analysis of how various parameters affect flow dynamics is provided. Future research in this area and the choice of machine learning as an efficient technique to predict micropolar flow will be supported by the current study.

Keywords: MHD, Blood flow, Stenotic artery, Sutterby fluid, Caputo time fractional derivative, Finite difference method.

1. Introduction

Experiments and theoretical studies of circulatory diseases are of interest to many researchers. It is evident today that smoking, severe hypercholesterolemia, modern lifestyle choices, and genetic disorders all contribute to artery blockage. A type of coronary artery disease called atherosclerosis arises due to the growth and collection of white blood cells in the arterial lumen. The accumulations cause the arterial wall to contract. This procedure also results in the formation of a plaque. Stenosis is the term used to describe the constriction of arteries caused through plaque formation. Several theoretical investigations have been conducted to examine how stenosis affects blood flow. Experimental research has demonstrated that human blood shows a double rheology. At low shear rates or under disease

*

conditions, a non-Newtonian character predominates, however blood exhibits a Newtonian nature at high shear rates. Bhatti et al. [1] concentrated on how non-Newtonian blood moves in a tapered stenosed artery. Blood rheological behaviour is classified most effectively using the Carreau fluid model. Behir et al. [2] studied the behaviour of blood flow in constricted arteries, focusing on its pulsing characteristics and variations in haemoglobin levels in three different medical conditions: normal health, diabetes, and anaemia. Owasit and Sriyab [3] investigated the power-law fluid's two-dimensional steady flow via asymmetric and vertically symmetric stenoses. Additionally, a lot of research has been done on how blood flows through stenosed arteries [4-6].

The extension of classical calculus, fractional calculus is used to handle non-integer order derivatives and integrals. It has found various significant applications in interesting fields such as heat transfer, fluid flow, and viscoelasticity theory [7]. Jamil et al. [8] examined blood flow via inclined, constricted artery under magnetic field effect. Time fractional derivative of Caputo-Fabrizio was used to formulate the governing equations. In a stenosed artery, Patel and Patel [9] considered fractional derivative model for blood dynamics. Precise description of the temperature fields, magnetic particle velocity, and blood velocity is obtained by expressing the governing set of equations in fractional time derivative form. Majeed et al. [10] observed the movement of blood through a cylindrical tube using fractional derivative. Moreover, Jamil et al. [11] studied non-Newtonian magnetic blood motion via inclined artery with thermal radiation using a fractional derivative model. Furthermore, by applying fractional derivatives, Tabi et al. [12] examined a mathematical representation of blood flow when magnetic particles are present. Additionally, Luqman et al. [13] evaluated OHAM's performance in analyzing the impact of thermal radiation and magnetic fields on blood flow in cylindrical arteries using fractional-order framework. Yakubu et al. [14] looked at how velocity of blood velocity as well as temperature distribution through circular cylindrical tube were affected by the Caputo time-fractional parameter.

A generalized Newtonian fluid model, the Sutterby fluid accurately depicts flow behaviour throughout a broad range of shear rates, including the region of zero-shear viscosity. It is particularly suited for representing high-polymer aqueous solutions. By adjusting its parameters, the Sutterby fluid model can capture both Newtonian and non-Newtonian fluid behaviors of complex flow dynamics. Kot and Elmabound [15] investigated the unsteady flow of a hybrid nanofluid, which is used to simulate blood, via mildly constricted artery. Blood is taken as Sutterby fluid in order to capture the effects of gyrotactic microorganism migration in the bloodstream, providing a more accurate understanding of complicated biofluid behavior. Raju et al. [16] focused on examining blood motion in two different stenosis arteries. Few core studies on MHD [16-18], non-Newtonian [19-24], blood flow [25-27] and Caputo fractional derivative [28-31] are referend to readers for the best understanding of topic under investigation.

Keeping above discussion in consideration, this research emphasizes Sutterby fluid passing through a narrowed vertical artery by considering magnetic field influences. Governing equations are derived in terms of cylindrical coordinates and solved numerically by using an explicit finite difference technique. A thorough analysis of significant physical parameters is pursued, and results are shown by graphical representations.

2. Problem Formulation

We considered the unsteady incompressible pulsatile blood motion in a vertically axisymmetric mild stenosed artery, Sutterby fluid is considered for analysis of blood flow through cylindrical coordinates (r, θ, z), where r is radial, θ is circumference, and z is flow direction. In axial direction, uniform external magnetic field is applied as shown in Figure 1.

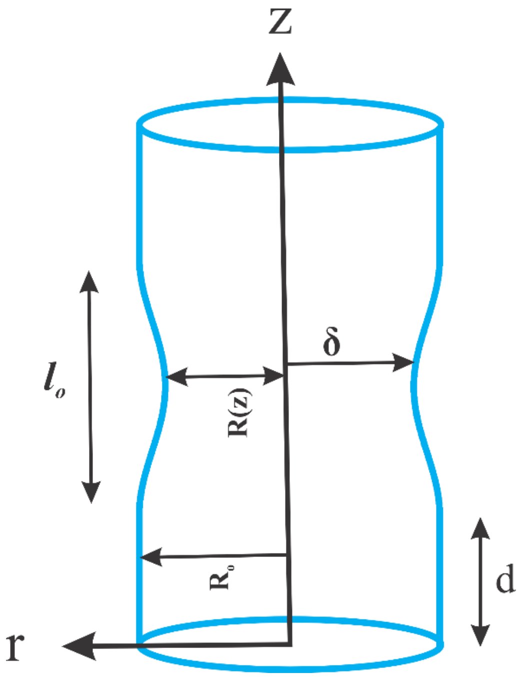

Fig.1: Geometry of the problem

Mathematically, the geometry of problem can be written as:

$$R(z) = \begin{cases} R_o - \frac{\delta}{2}\left(1 + \text{Cos}\left(\frac{2\pi}{l_o}\right)\left(\bar{z} - \bar{d} - \left(\frac{l_o}{2}\right)\right)\right), \bar{d} \leq \bar{z} \leq \bar{d} + l_o, \\ R_o \qquad\qquad\qquad\qquad \text{otherwise.} \end{cases} \tag{1}$$

.

In Eq. (1), R_o is the artery radius, $\bar{z}$ is the axial coordinate, distance from origin is $\bar{d}$, height of stenosis is expressed by δ, whereas l_o denotes stenosis length. Due to axisymmetric flow, the circumferential direction is neglected.

Let $\boldsymbol{V} = \left[\bar{u}(r,z,t), 0, \bar{w}\,(r,z,t)\right]$, be the velocity filed, in which $\bar{u}$ and $\bar{w}$ are radial and axial directions of velocity respectively. In view of Cauchy stress tensor [32], nondimensional variables [33] along with hypotheses $\frac{R_o}{l_o} \approx O(1)$ and $\frac{\delta^*}{R_o} \ll 1$, by neglecting the higher power terms (i.e., $(\gamma B)^3, (\gamma B)^4, \ldots$), the resulting equations along with the geometry of the problem in dimensionless form are:

$$\frac{\partial w}{\partial z} = 0, \tag{2}$$

$$\frac{\partial p}{\partial r} = 0, \tag{3}$$

$$Re\frac{\partial w}{\partial t} = -\frac{\partial P}{\partial z} + \frac{1}{r}\frac{\partial}{\partial r}\left(r\left(\epsilon_1\frac{\partial w}{\partial r} - m\epsilon_2\left(\frac{\partial w}{\partial r}\right)^3\right)\right) + G_r\theta - M_a^2 w \quad , \tag{4}$$

$$\frac{\partial\theta}{\partial t} = \frac{1}{\Pr Re}\left(\frac{1}{r}\frac{\partial\theta}{\partial r} + \frac{\partial^2\theta}{\partial r^2}\right) + \frac{Nr}{\Pr Re}\frac{\partial^2\theta}{\partial r^2} + \frac{Ec\, M_a^2}{Re}w^2 \quad , \tag{5}$$

$$S_{rz} = \left(\epsilon_1\frac{\partial w}{\partial r} - m\epsilon_2\left(\frac{\partial w}{\partial r}\right)^3\right) \quad . \tag{6}$$

$$\frac{\partial P}{\partial z} = -B_1\left(1 + e\cos(2\pi t)\right) \quad . \tag{7}$$

$$R(z) = \begin{cases} 1 - \frac{\delta^*}{2}\left(1 + Cos2\pi\left(z - d - \frac{1}{2}\right)\right), & d \le z \le d+1 \\ 1, & \text{otherwise} \end{cases} \quad . \tag{8}$$

where steady state pressure gradient is A_o , pressure oscillation that raises systolic and diastolic pressures is A_1, and ω_p represents pulse rate frequency.

The shear thinning property $(\gamma B \ll 1)$ [34] is as follows:

$$\gamma B - \frac{(\gamma B)^3}{6} \cong sinh^{-1}(\gamma B) \quad . \tag{9}$$

In view of radial coordinate transformation $\left(\xi = \frac{r}{R(z)}\right)$, the resulting equations take the following forms:

$$Re\frac{\partial w}{\partial t} = B_1\left(1 + e\cos(2\pi t)\right) + \frac{1}{\xi R^2}\frac{\partial}{\partial \xi}\left(\xi\left(\epsilon_1\frac{\partial w}{\partial \xi} - \frac{m\epsilon_2}{R^2}\left(\frac{\partial w}{\partial \xi}\right)^3\right)\right) + G_r\theta - M_a^2 w \tag{10}$$

$$\frac{\partial\theta}{\partial t} = \frac{1}{\Pr R^2 Re}\left(\frac{1}{\xi}\frac{\partial\theta}{\partial \xi} + \frac{\partial^2\theta}{\partial \xi^2}\right) + \frac{Nr}{\Pr R^2 Re}\frac{\partial^2\theta}{\partial \xi^2} + \frac{Ec\, M_a^2}{Re}w^2 \quad . \tag{11}$$

Here, $P, k, \rho, T, \alpha, \mu, g, t, B_o, C_p, \sigma,$ and β denote pressure, thermal conductivity, density, temperature, inclination angle, dynamic viscosity, gravitational force, time, magnetic field strength, specific heat at constant pressure, electrical conductivity, and thermal expansion coefficient, respectively.

By applying Caputo time fractional derivative on momentum and energy equations, we have

$$ReD_t^{\alpha} w = B_1(1 + e\cos(2\pi t)) + \frac{1}{\xi R^2}\frac{\partial}{\partial \xi}\left(\xi\left(\epsilon_1\frac{\partial w}{\partial \xi} - \frac{m\epsilon_2}{R^2}\left(\frac{\partial w}{\partial \xi}\right)^3\right)\right) + G_r\theta - M_a^2 w, \tag{12}$$

$$D_t^{\alpha}\theta = \frac{1}{\Pr R^2 Re}\left(\frac{1}{\xi}\frac{\partial \theta}{\partial \xi} + \frac{\partial^2\theta}{\partial \xi^2}\right) + \frac{Nr}{\Pr R^2 Re}\frac{\partial^2\theta}{\partial \xi^2} + \frac{Ec\, M_a^2}{Re}w^2 \quad . \tag{13}$$

Where D_t^{α} represent Caputo time-fractional derivative, addressed by Shah et al. [35]:

$$D_t^{\gamma}u(r,t) = \begin{cases} \frac{1}{\Gamma(1-\gamma)}\int_0^t \frac{1}{(t-\tau)^{\gamma}}\frac{\partial u(r,\tau)}{\partial \tau}d\tau, & 0<\gamma<1, \\ \frac{\partial u(r,\tau)}{\partial \tau}, & \gamma = 1 . \end{cases} \tag{14}$$

The associated boundary conditions are:

$$w(\xi,0) = 0, \theta(\xi,0) = 0, \text{at } t = 0 \quad , \tag{15}$$

$$\frac{\partial w(0,t)}{\partial \xi} = 0, \frac{\partial \theta(0,t)}{\partial \xi} = 0, at\ \xi = 0 \quad , \tag{16}$$

$$w(1,t) = 0, \theta(1,t) = 1,\ at\ \xi = 1 \ . \tag{17}$$

The wall shear stress, flow rate, and resistance to flow for Sutterby fluid model are:

$$\tau_s = \left(\frac{\epsilon_1}{R}\frac{\partial w}{\partial \xi} - \frac{m\epsilon_2}{R^3}\left(\frac{\partial w}{\partial \xi}\right)^3\right)_{\xi=1} \quad . \tag{18}$$

$$Q_F = R^2 2\pi\int_0^1 w\,\xi\, d\xi \ . \tag{19}$$

$$\lambda = \frac{L\left(\frac{\partial P}{\partial z}\right)}{Q_F} \ . \tag{20}$$

The classical Sutterby fluid model can be recovered by taking $\gamma = 1$.

3. Finite difference approximation

Finding an analytical solution of these equations is difficult because of their high nonlinearity and complex boundary conditions. Hence, a numerical method [36] is used to solve this problem. Forward difference and central difference methods are utilized to approximate partial derivatives in time and space.

$$\frac{\partial w}{\partial t} \cong \frac{w_{i,j+1} - w_{i,j}}{\Delta t} \quad , \tag{21}$$

$$\frac{\partial w}{\partial \xi} \cong \frac{w_{i+1,j} - w_{i-1,j}}{2\Delta\xi} \quad , \tag{22}$$

$$\frac{\partial^2 w}{\partial \xi^2} \cong \frac{w_{i+1,j} - 2w_{i,j} + w_{i-1,j}}{\Delta\xi^2} \quad , \tag{23}$$

$$D_t^{\alpha} w = \frac{1}{\Gamma(1-\gamma)} \sum_{j=0}^{k} \int_{t_j}^{t_{j+1}} \frac{\partial w(\xi,\eta)}{\partial \eta} \frac{d\eta}{(t_{k+1}-\eta)^{\gamma}} = \frac{1}{\Gamma(1-\gamma)} \sum_{j=0}^{k} \frac{w_{i,j+1} - w_{i,j}}{\Delta t} \int_{t_j}^{t_{j+1}} \frac{d\eta}{(t_{k+1}-\eta)^{\gamma}},$$

$$\frac{1}{\Gamma(1-\gamma)} \sum_{j=0}^{k} \frac{w_{i,j+1} - w_{i,j}}{\Delta t} \int_{t_j}^{t_{j+1}} \frac{d\eta}{(t_{k+1}-\eta)^{\gamma}} = \frac{1}{\Gamma(1-\gamma)} \sum_{j=0}^{k} \frac{w_{i,k+1-j} - w_{i,k-j}}{\Delta t} \int_{t_{k-j}}^{t_{k+1-j}} \frac{d\zeta}{(\zeta)^{\gamma}} \tag{24}$$

$$= \frac{1}{\Gamma(2-\gamma)} \sum_{j=0}^{k} \frac{w_{i,k+1-j} - w_{i,k-j}}{\Delta t^{\gamma}} c_j = \frac{\Delta t^{-\gamma}}{\Gamma(2-\gamma)} \left[w_{i,k+1} - w_{i,k} + \sum_{j=1}^{k} \left(w_{i,k+1-j} - w_{i,k-j} \right) c_j \right]$$ (25

Where $c_j = (j+1)^{1-\gamma} - (j)^{1-\gamma}$, $c_0 = 1$

Now, put these values of the fractional derivative in the momentum and energy equations:

$$Re \frac{\Delta t^{-\gamma}}{\Gamma(2-\gamma)} \left[w_{i,k+1} - w_{i,k} + \sum_{j=1}^{k} \left(w_{i,k+1-j} - w_{i,k-j} \right) c_j \right] = B_1 \left(1 + e \cos\left(2\pi t_k \right) \right) + \frac{1}{\xi_i R^2} \frac{\partial}{\partial \xi} \left(\xi_i \left(\epsilon_1 w_{\xi} - \frac{m\epsilon_2}{R^2} \left(w_{\xi} \right)^3 \right) \right) + G_r \theta_{i,k} - M_a^2 w_{i,k} \tag{26}$$

$$\frac{\Delta t^{-\gamma}}{\Gamma(2-\gamma)} \left[\theta_{i,k+1} - \theta_{i,k} + \sum_{j=1}^{k} \left(\theta_{i,k+1-j} - \theta_{i,k-j} \right) c_j \right] = \frac{1}{\Pr R^2 Re} \left(\frac{1}{\xi_i} \theta_{\xi} + \theta_{\xi\xi} \right) + \frac{Nr}{\Pr R^2 Re} \theta_{\xi\xi} + \frac{Ec\, M_a^2}{Re} w_{i,k}^{\;2} \tag{27}$$

With boundary conditions are:

$$w_i^1 = \theta_i^1 = 0 \text{ when } t = 0 , \tag{28}$$

$$w_{N+1}^k = w_N^k, \theta_{N+1}^k = \theta_N^k \text{ when } \xi = 0 , \tag{29}$$

$$w_{N+1}^k = 0, \theta_{N+1}^k = 1 \text{ when } \xi = 1 . \tag{30}$$

When choosing a step-size, stability of this scheme can be determined by following:

$$\Delta t \le \frac{(\Delta\xi)^2}{2\, Re} \tag{31}$$

Stability of numerical method depends on chosen space and time steps. Criteria are satisfied at $\Delta\chi = 0.025$ and $\Delta t = 0.00001.$

4. Results and Discussion

Graphs for velocity, wall shear stress, flow rate, and resistance to flow are generated using a MATLAB program. These plots help to explain the physical behavior of the system being studied. The following values are used to explore how different parameters affect blood dynamics.
$B_1 = 2; Ec = 0.5; e = 0.5; m = 2; \delta = 0.1; Pr = 21; L = 2; Ma = 5; \varepsilon_1 = 2.5; R_0 = 1; d = 0.5; Re = 5; \alpha = 0.7; Gr = 0.5; \varepsilon_2 = 0.1; z = 0.77; Nr = 1$

In Figs. (2) and (3), the behavior is governed by the fractional derivative, which captures the memory of the fluid. Simplistically, the fluid "remembers" its history of motion, and this influences its flow. It is observed that when the fractional parameter α is larger, the fluid behaves more like a classical fluid with reduced memory, thus reacting to changes more quickly. Consequently, velocity and wall shear stress increase slightly. The increase and decrease in the graphs reflect fluid flow over time—first dropping, then rising, and eventually dropping again. This cycle occurs as a result of the balance between fluid inertia, viscous resistance, and the memory effect introduced by the fractional model.
The temperature profile influenced by the fractional parameter is shown in Fig. (4). Initially, temperature decreases because fluid velocity is lower in the constricted region, which results in less friction and fewer collisions between fluid particles and with the artery wall. This reduces the heat generated in the blood. As time progresses and the blood overcomes the resistance from the stenosis, the flow becomes smoother with higher velocity. This enhances the rate of collisions between particles and with the artery wall, leading to increased heat due to friction, which raises the temperature, particularly near the arterial wall.

Fig. (5) shows the dependence of blood velocity on the Grashof number (Gr), which represents the ratio of thermal buoyancy to viscous resistance. As Gr increases, thermal forces dominate and enhance momentum transfer, resulting in higher overall fluid velocity. This illustrates how stenosis in the artery wall affects arterial blood flow. With an increase in Gr, thermal buoyancy raises the velocity near the arterial wall. As a result, both flow rate Q and shear stress τ increase, as illustrated in Figs. (6) and (7), respectively. The opposite behavior is observed in Fig. (8) for the case of flow resistance. As the Hartmann number Ma increases, indicating stronger magnetic field influence, the magnetic effect (known as the Lorentz force) acts like a drag on the flowing blood, slowing it down. Consequently, velocity, flow rate, shear stress, and resistance to flow decrease, as shown in Figs. (9)–(12). Overall, Q drops because circulation of blood is slowed by magnetic resistance. As a result, λ increases, making it more difficult for blood to pass through the narrowed parts of the artery.
Figs. (13) and (14) illustrate the effect of ϵ_1 and ϵ_2 on velocity along the arterial blood vessel and on flow rate. Increasing the value of ϵ_1 reduces blood axial velocity, whereas increasing ϵ_2 enhances the flow rate. The reduction in velocity with higher ϵ_1 demonstrates the viscoelastic behavior of blood. Figs. (15) and (16) show wall shear stress and resistance to flow against ϵ_1, while Figs. (17)–(20) illustrate how ϵ_2 affects velocity, shear stress, flow rate, and resistance to flow. It can be seen that τ increases with higher ϵ_1, but decreases with higher ϵ_2. Since Q and λ are inversely proportional, an increase in ϵ_1 reduces Q and increases λ, while the opposite behavior is seen for ϵ_2.
In Fig. (21), the influence of thermal radiation on temperature within a stenosed artery is displayed. It is noted that as Nr increases, temperature rises due to enhanced radiative heat transfer, which increases thermal diffusivity by contributing more thermal energy to the system. This rise in temperature can also indirectly increase momentum diffusivity by lowering fluid viscosity.
The effect of the Eckert number Ec on temperature is shown in Fig. (22). Ec accounts for the

transformation of kinetic energy into internal energy due to viscous dissipation. When Ec increases, it indicates that blood velocity is high enough for frictional heating to become significant. As blood passes through the narrowed region of an artery, resistance and shear forces are elevated due to the reduced cross-sectional area. This intensifies viscous effects, especially for non-Newtonian fluids. The energy dissipated from internal friction is transformed into heat energy, causing the blood temperature to rise.

5. Conclusion

The present research provides a detailed investigation of blood motion through a constricted artery using a fractional derivative model, which incorporates the memory effect in blood dynamics. MATLAB-based simulations were employed to examine the key characteristics of the flow under the influence of significant physical parameters. The fractional model demonstrates how the memory of past motion strongly influences blood behavior, making the study more realistic than classical models.

1. The variations in τ, velocity, and Q with increasing fractional order α show a clear trend: they first decrease and then increase. This occurs due to the balance between fluid memory, inertia, and resistance in the narrowed artery. At lower α, strong memory slows the flow, whereas higher α makes the fluid behave more like a Newtonian fluid, thereby improving flow.

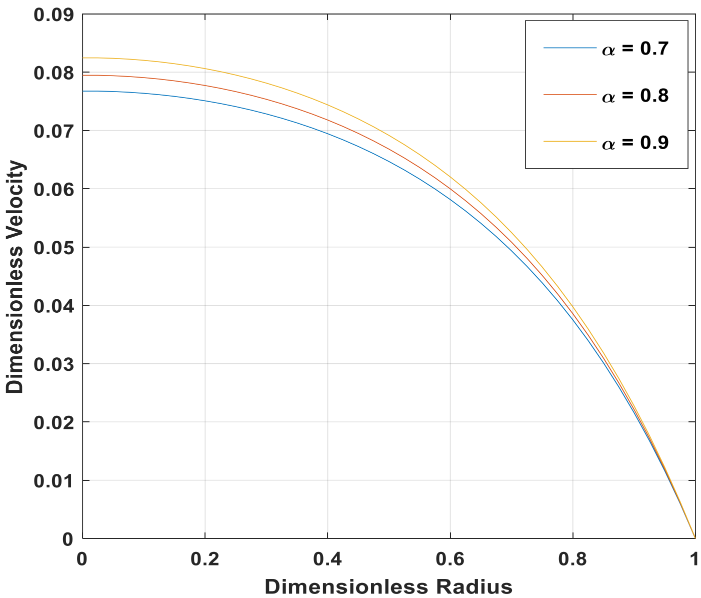

Fig.2: Velocity profile at t = 1.2 for α.

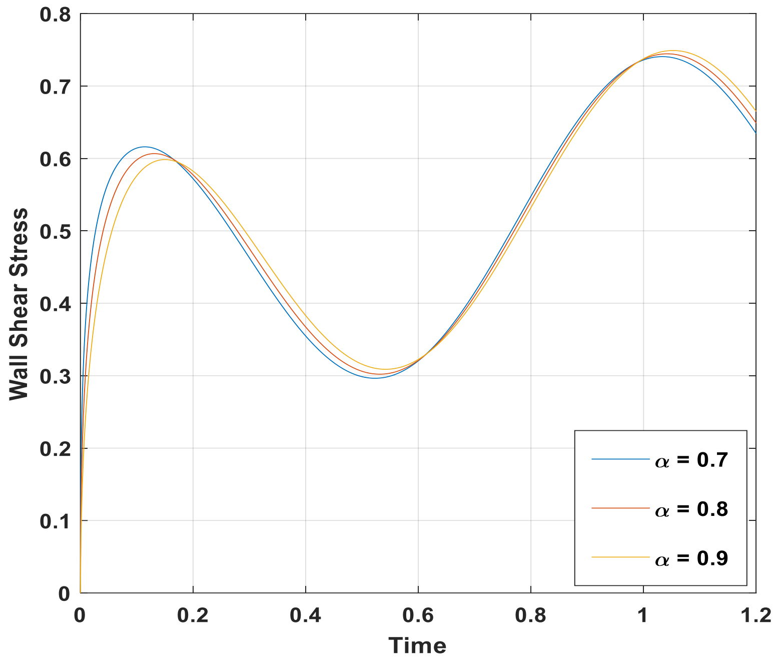

Fig. 3: Wall shear stress for α.

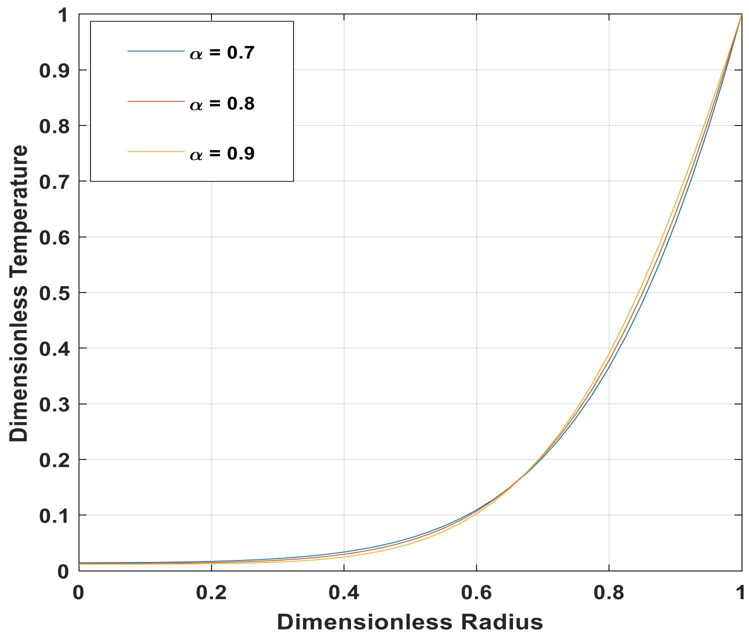

Fig.4: Temperature profile at t = 1.2 for α.

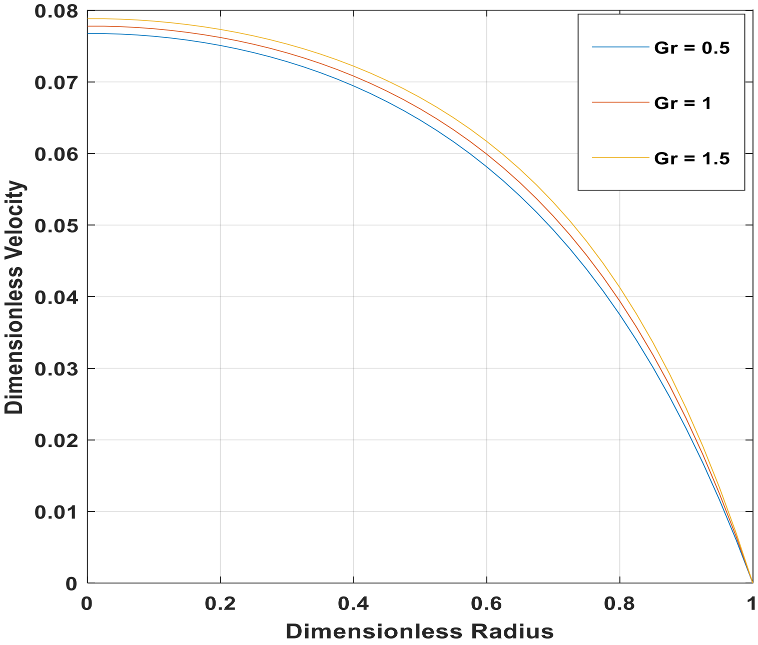

Fig.5: Velocity profile at t = 1.2 for Gr .

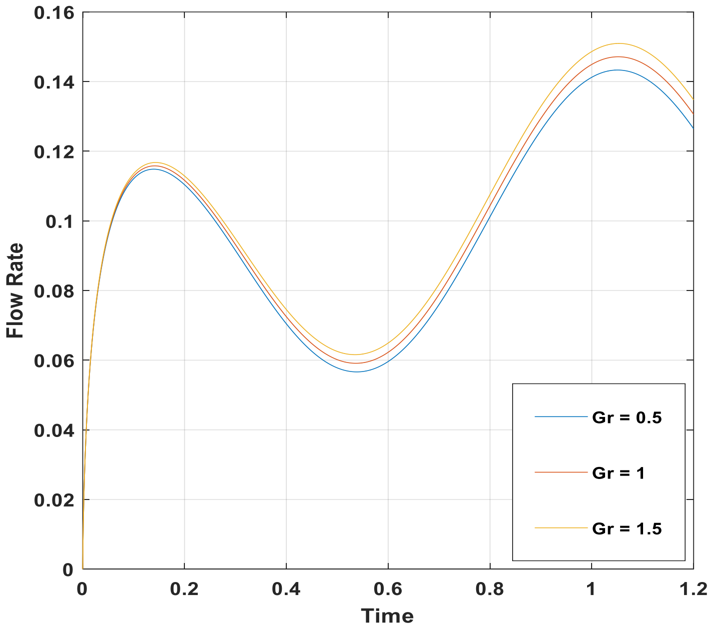

Fig.6: Flow rate for Gr

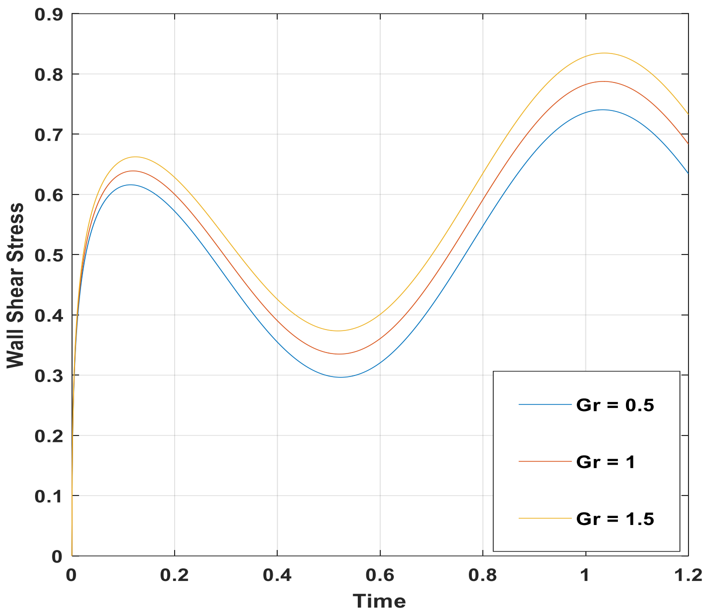

Fig.7: Wall shear stress for Gr

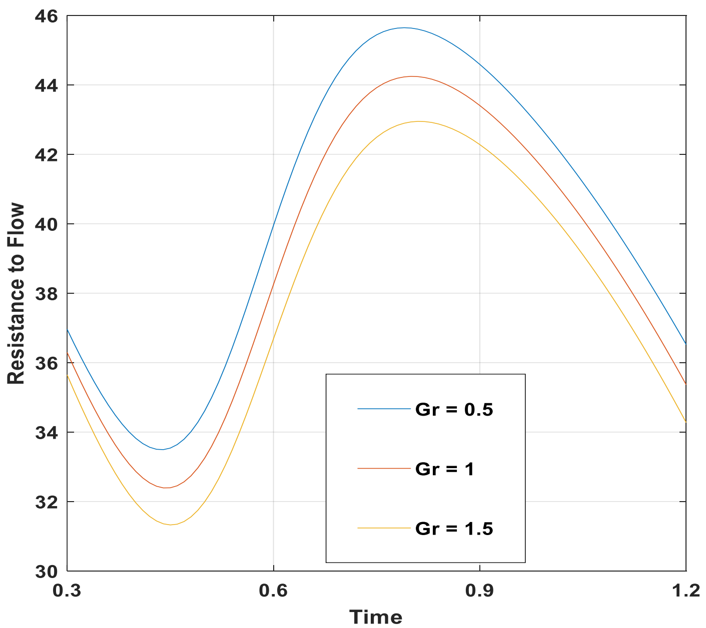

Fig. 8: Resistance to flow for Gr

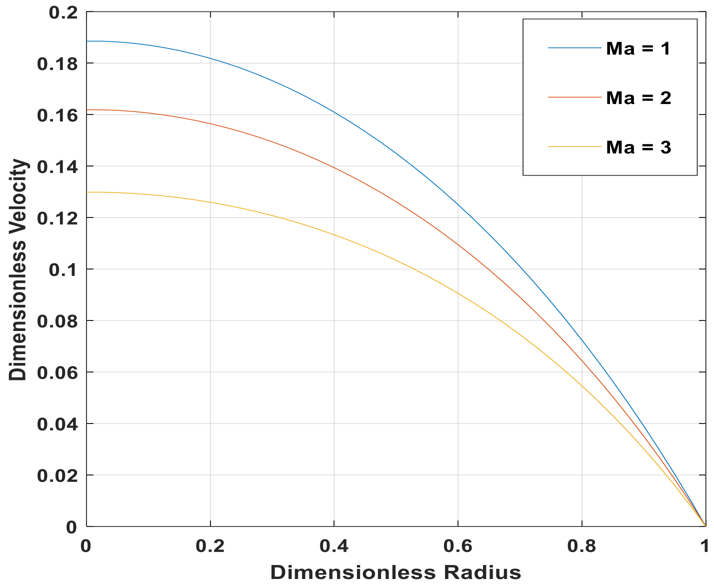

Fig.9: Velocity profile at t = 1.2 for Ma.

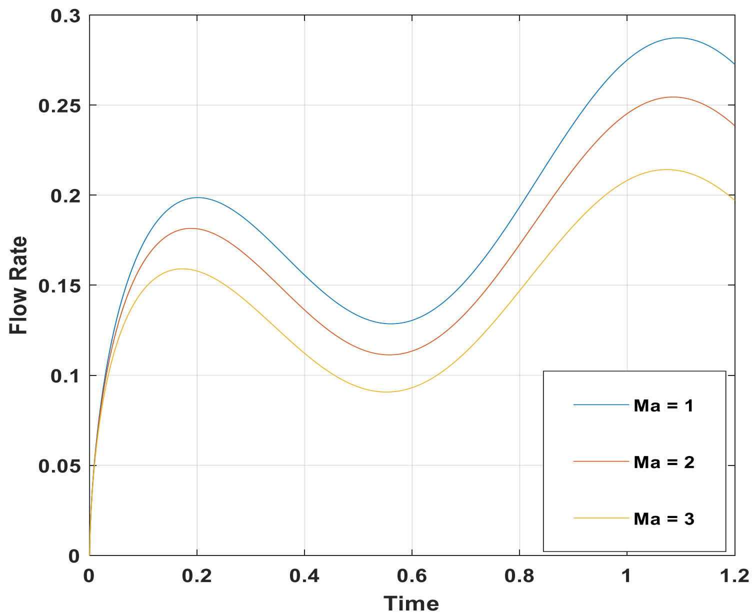

Fig.10: Flow rate for Ma.

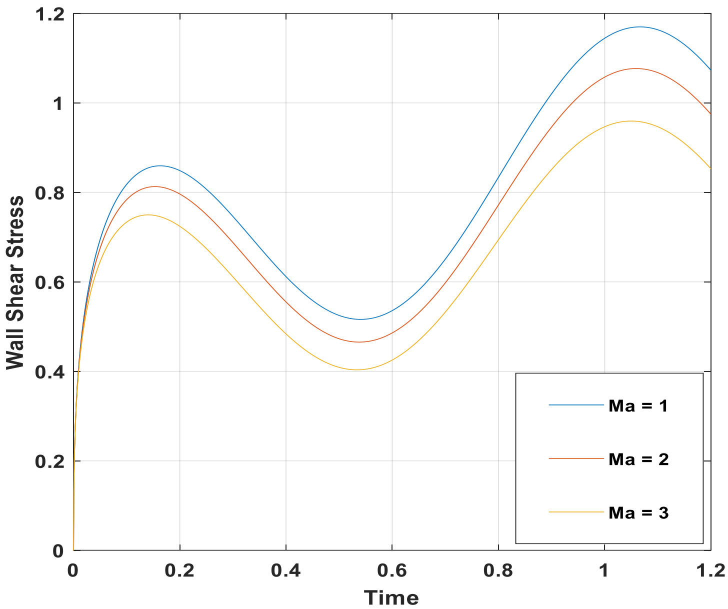

Fig.11: Wall shear stress for Ma.

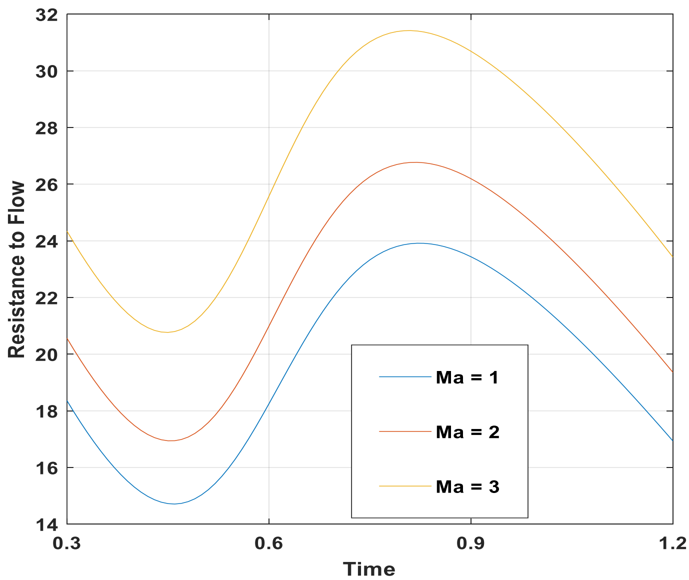

Fig.12: Resistance to flow for Ma.

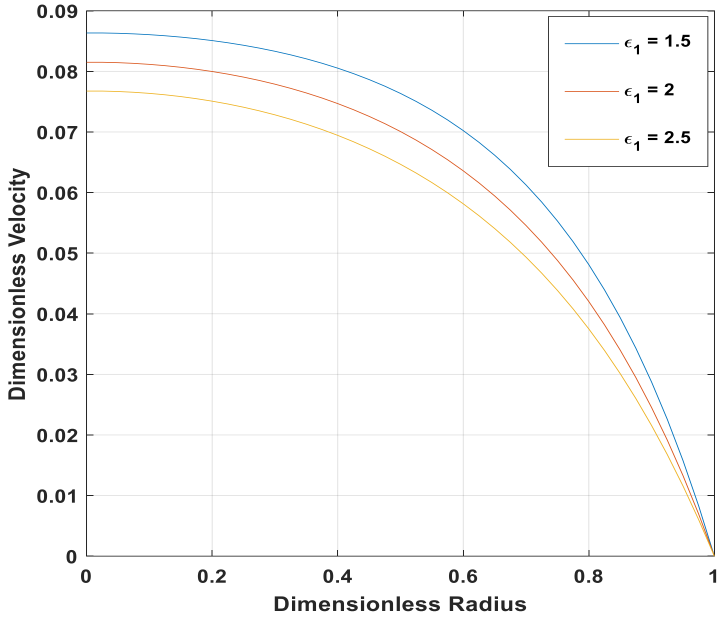

Fig.13: Velocity profile at t = 1.2 for ϵ_1 .

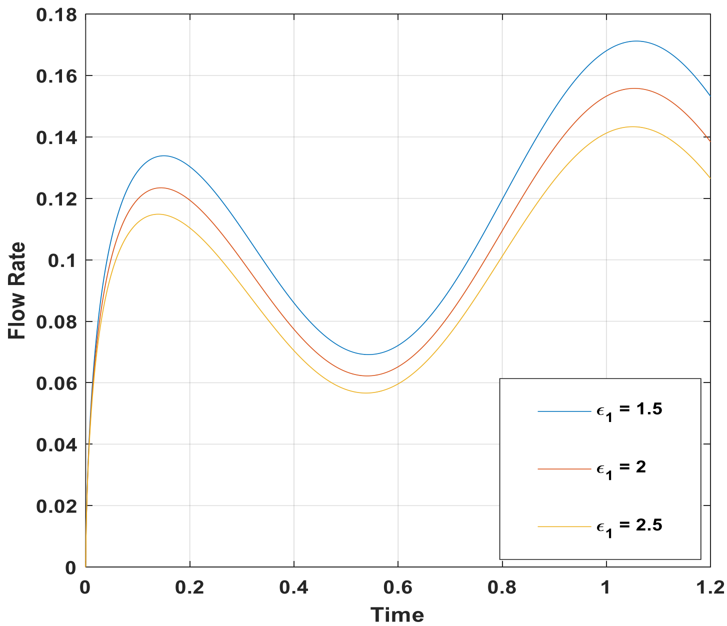

Fig.14: Flow rate for ϵ_1 .

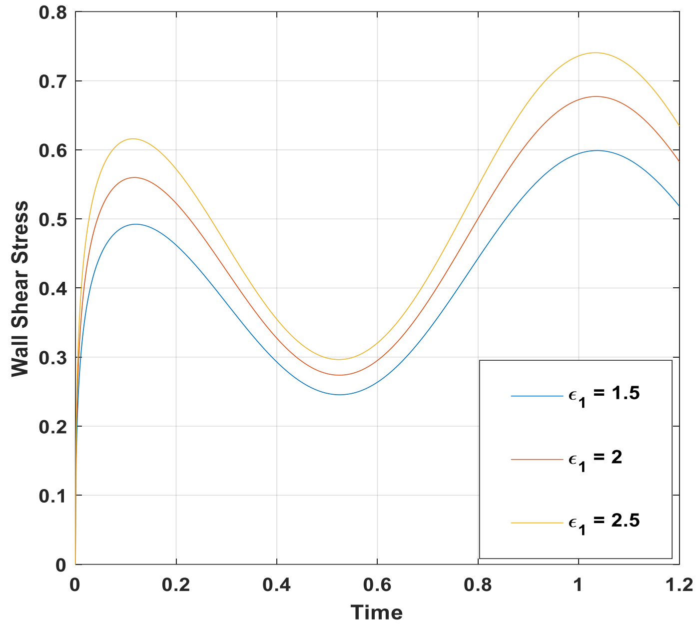

Fig.15: Wall shear stress for ϵ_1 .

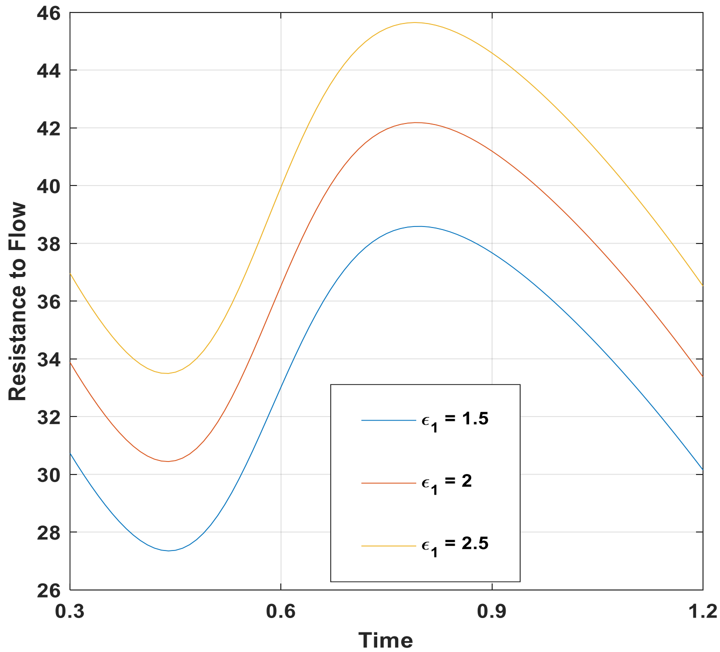

Fig.16: Resistance to flow for ϵ_1 .

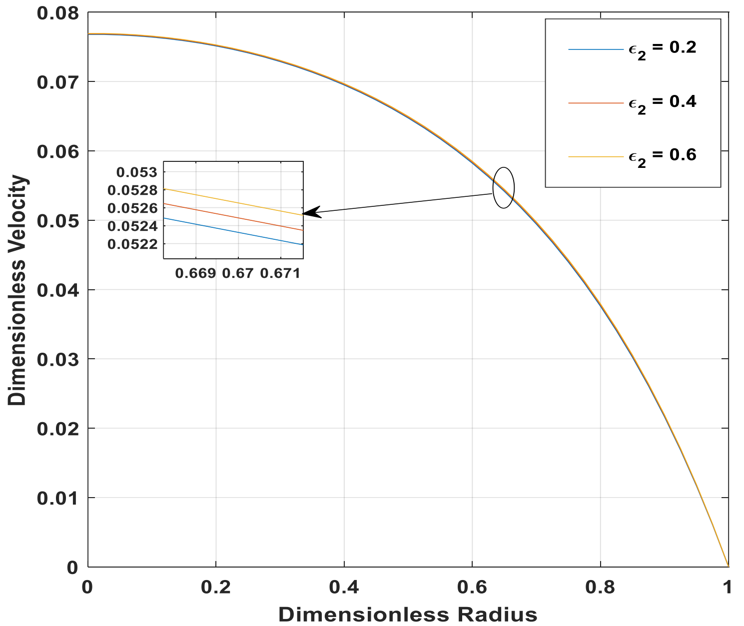

Fig.17: Velocity profile at t = 1.2 for ϵ_2 .

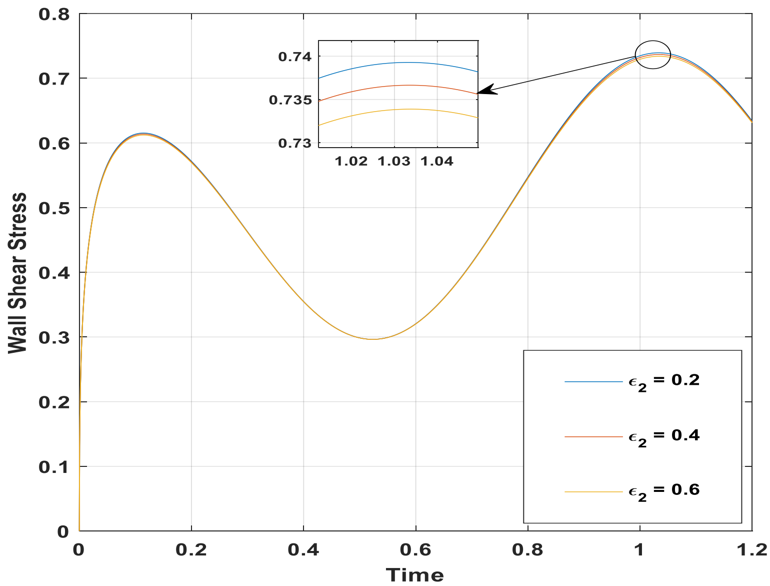

Fig.18: Wall shear stress for ϵ_2 .

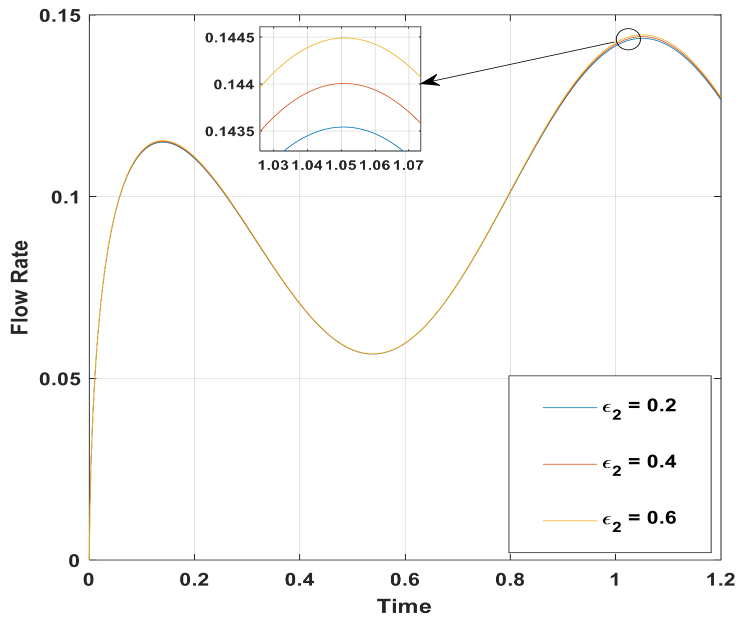

Fig.19: Flow rate for ϵ_2 .

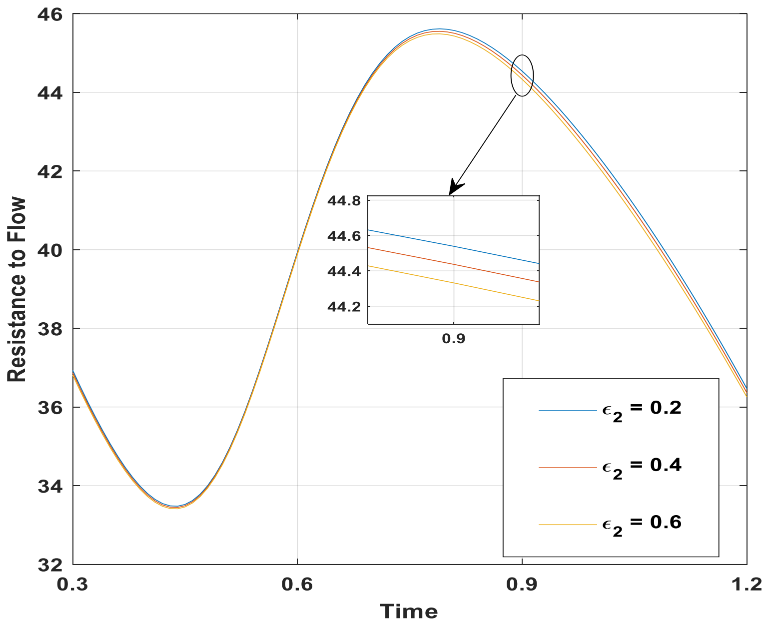

Fig.20: Resistance to flow for ϵ_2 .

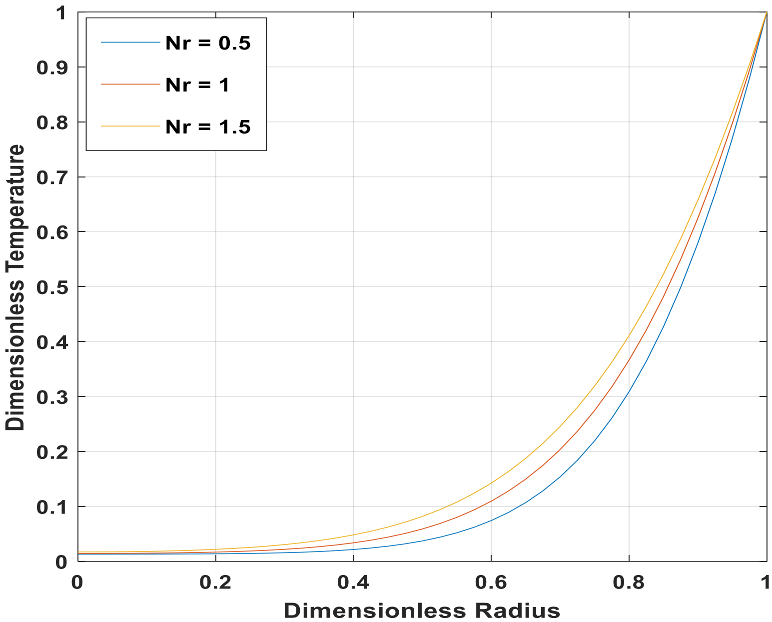

Fig.21: Temperature profile at t = 1.2 for Nr.

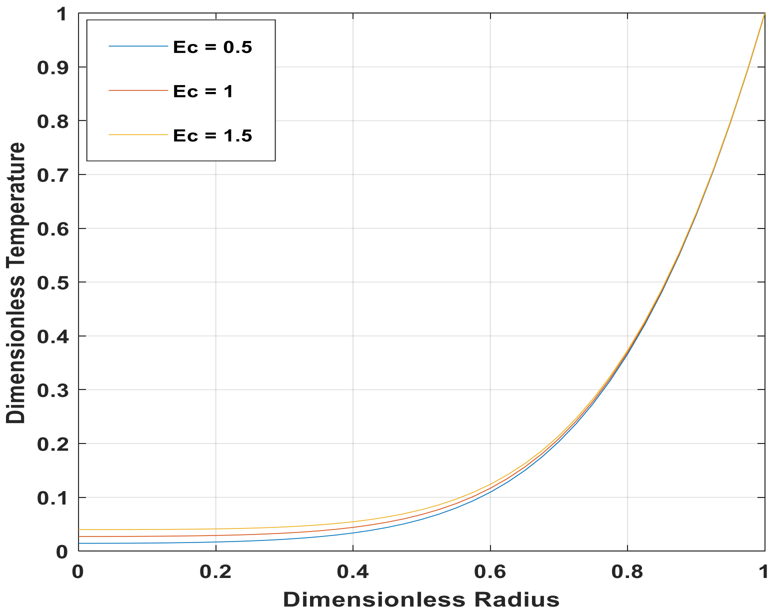

Fig.22: Temperature profile at t = 1.2 for Ec .

1. An increase in the Grashof number Gr leads to higher velocity, Q, and τ, as greater thermal buoyancy enhances momentum transfer.
2. A rise in the Hartmann number Ma introduces stronger magnetic resistance, which reduces both blood velocity and flow rate.

3. Increasing ϵ_1 decreases velocity and flow rate while increasing wall shear stress and resistance, reflecting the viscoelastic behavior of blood. In contrast, increasing ϵ_2 enhances velocity and flow rate but reduces resistance and shear stress.
4. Parameters such as the radiation parameter Nr and the Eckert number (Ec) have a significant impact on the temperature profile. Larger values of Nr and Ec increase blood temperature due to radiative heat transfer and viscous dissipation, respectively.
5. This research has important implications for medical professionals, especially regarding what determines blood flow in diseased arteries under different physiological conditions. It is able to predict complications in arterial stenosis patients and inform improved treatment strategies, such as thermal therapies or using magnetic field for treatments. For future development, the model can be further improved using machine learning methods to predict automatically flow patterns, identify abnormalities, and find optimal parameter values for various patient profiles. Furthermore, comparing this model to other fractional derivatives models can provide greater understanding of how various memory kernels affect flow behavior towards more precise and patient-specific models.

References

[1] M. M. Bhatti, S. M. Sait, R. Ellahi, Magnetic nanoparticles for drug delivery through tapered stenosed artery with blood based non-Newtonian fluid, *Pharmaceuticals,* Vol. 15, No. 11, pp. 1352, 2022.

[2] B. Behir, A. Benslimane, H. Mehdaoui, B. Mehdi, Impact of hematocrit on pulsatile blood flow in stenosed arteries: a computational study in healthy, diabetic, and anemic models, *Comput Methods Biomech Biomed Engin,* Vol. 28, No. 6, pp. 764-776, May, 2025. eng

[3] P. Owasit, S. Sriyab, Mathematical modeling of non-Newtonian fluid in arterial blood flow through various stenoses, *Advances in Difference Equations,* Vol. 2021, No. 1, pp. 340, 2021/07/16, 2021.

[4] A. Elelamy, N. Elgazery, R. Ellahi, Blood flow of MHD non-Newtonian nanofluid with heat transfer and slip effects: Application of bacterial growth in heart valve, *International Journal of Numerical Methods for Heat & Fluid Flow,* Vol. ahead-of-print, 03/05, 2020.

[5] A. A. Khan, S. Z. Satti, R. Ellahi, S. M. Sait, Heat transfer analysis on peristaltically driven motion of particle-fluid suspension in Newtonian fluid using curvilinear coordinates bounded by slip boundary: Applications in drug delivery through blood vessels, *International Communications in Heat and Mass Transfer,* Vol. 167, pp. 109362, 2025/09/01/, 2025.

[6] J. Prakash, D. Tripathi, A. K. Tiwari, S. M. Sait, R. Ellahi, Peristaltic Pumping of Nanofluids through a Tapered Channel in a Porous Environment: Applications in Blood Flow, *Symmetry,* Vol. 11, No. 7, pp. 868, 2019.

[7] X. Wang, Y. Qiao, H. Qi, H. Xu, Numerical study of pulsatile non-Newtonian blood flow and heat transfer in small vessels under a magnetic field, *International Communications in Heat and Mass Transfer,* Vol. 133, pp. 105930, 2022/04/01/, 2022.

[8] D. F. Jamil, S. Saleem, R. Roslan, F. S. Al-Mubaddel, M. Rahimi-Gorji, A. Issakhov, S. U. Din, Analysis of non-Newtonian magnetic Casson blood flow in an inclined stenosed artery using Caputo-Fabrizio fractional derivatives, *Comput Methods Programs Biomed,* Vol. 203, pp. 106044, May, 2021. eng

[9] H. Patel, N. Patel, Study of fractional-order model on Casson blood flow in stenosed artery with magnetic field effect, *Waves in Random and Complex Media*, pp. 1-19, 2023.

[10] S. Majeed, F. Ali, A. Imtiaz, I. Khan, M. Andualem, Fractional model of MHD blood flow in a cylindrical tube containing magnetic particles, *Scientific Reports,* Vol. 12, 01/10, 2022.

[11] D. F. Jamil, S. Uddin, M. Kazi, R. Roslan, M. R. Gorji, M. Kamalrulzaman Md Akhir, MHD blood flow effects of Casson fluid with Caputo-Fabrizio fractional derivatives through an inclined blood vessels with thermal radiation, *Heliyon,* Vol. 9, No. 11, pp. e21780, Nov, 2023. eng

[12] C. B. Tabi, P. A. Ndjawa Yomi, T. Motsumi, C. Kamdem, T. C. Kofane, Magnetic field effect on a fractionalized blood flow model in the presence of magnetic particles and thermal radiations, *Chaos Solitons & Fractals,* Vol. 131, 11/28, 2019.

[13] M. Luqman, S. Iqbal, H. Younas, J. Ali, N. Ahmed, A. Akgül, An efficient computational approach for fractional model of blood flow in oscillatory arteries with thermal radiation and magnetic field effects, *Available at SSRN 4313039*, 2020.

[14] G. Yakubu, M. Abdulhameed, G. Adamu, U. Hassan, M. Kaurangini, Construction of the exact solution of blood flow of oldroyd-B fluids through arteries with effects of fractional derivative magnetic field and heat transfer, *Journal of Mechanics in Medicine and Biology,* Vol. 22, 08/18, 2022.

[15] M. El Kot, Y. Elmaboud, Numerical Simulation of Electroosmotic Sutterby Hybrid Nanofluid Flowing Through an Irregularly Mild Stenotic Artery with an Aneurysm, *Arabian Journal for Science and Engineering,* Vol. 49, 09/14, 2023.

[16] C. S. K. Raju, H. T. Basha, N. F. M. Noor, N. A. Shah, S.-J. Yook, Significance of body acceleration and gold nanoparticles through blood flow in an uneven/composite inclined stenosis artery: A finite difference computation, *Mathematics and Computers in Simulation,* Vol. 215, pp. 399-419, 2024/01/01/, 2024.

[17] A. Khan, S. Noor, R. Ellahi, S. Sait, THERMAL ANALYSIS OF TWO-PHASE MHD FLOW DUE TO CILIARY MOVEMENT WITH VISCOUS DISSIPATION IN THE PRESENCE OF HEAT SOURCE/SINK, *Journal of Enhanced Heat Transfer*, 01/01, 2025.

[18] J. Mehboob, R. Ellahi, S. M. Sait, N. S. Akbar, Optimizing bioconvective heat transfer with MHD Eyring–Powell nanofluids containing motile microorganisms with viscosity variability and porous media in ciliated microchannels, *International Journal of Numerical Methods for Heat & Fluid Flow,* Vol. 35, No. 2, pp. 825-846, 2025.

[19] R. Ellahi, S. Alamri, A. Majeed, Effects of MHD and slip on heat transfer boundary layer flow over a moving plate based on specific entropy generation, *Journal of Taibah University for Science,* Vol. 12, pp. 1-7, 06/14, 2018.

[20] S. M. Sait, R. Ellahi, N. Khalid, T. Taha, A. Zeeshan, Effects of thermal radiation on MHD bioconvection flow of non-Newtonian fluids using linear regression based machine learning and artificial neural networks, *International Journal of Numerical Methods for Heat & Fluid Flow,* Vol. 35, No. 5, pp. 1587-1609, 2025.

[21] R. Ellahi, N. Khalid, A. Zeeshan, S. Sait, M. Imran Khan, Heat transfer flow of non-Newtonian eyring-powell fluid with mixed convection heterogeneous and homogeneous reactions using linear regression based machine learning approach, *Machine Learning,* Vol. 114, 04/29, 2025.

[22] M. S. Nadeem, A. Zeeshan, A. Majeed, S. M. Sait, R. Ellahi, Cavitating bubbly flow of non-Newtonian second grade fluid through nozzles: Application of reduction of cavitation damage and noise, *International Journal of Modern Physics B,* Vol. 39, No. 11, pp. 2550085, 2025.

[23] M. M. Bhatti, A. Zeeshan, F. Bashir, S. M. Sait, R. Ellahi, Sinusoidal motion of small particles through a Darcy-Brinkman-Forchheimer microchannel filled with non-Newtonian fluid under electro-osmotic forces, *Journal of Taibah University for Science,* Vol. 15, No. 1, pp. 514-529, 2021/01/01, 2021.

[24] F. Ishtiaq, R. Ellahi, Thermomagnetic mucociliary transport of cilia-driven flow of non-Newtonian Bingham–Papanastasiou fluid under quadratic convection and joule heating effects in a porous respiratory channel, *International Communications in Heat and Mass Transfer,* Vol. 169, pp. 109674, 2025/12/01/, 2025.

[25] M. Dhange, G. C. Sankad, R. Safdar, D.-W. Jamshed, M. Eid, U. Bhujakkanavar, S. Gouadria, R. Chouikh, A mathematical model of blood flow in a stenosed artery with post-stenotic dilatation and a forced field, *PLOS ONE,* Vol. 17, pp. e0266727, 07/01, 2022.

[26] M. A. Kabir, M. F. Alam, M. A. Uddin, Numerical simulation of pulsatile blood flow: a study with normal artery, and arteries with single and multiple stenosis, *Journal of Engineering and Applied Science,* Vol. 68, No. 1, pp. 24, 2021/11/07, 2021.

[27] M. Shahzad, N. Ahammad, S. Nadeem, S. Allahyani, E. Tageldin, A. Awan, Sensitivity analysis for Rabinowitsch fluid flow based on permeable artery constricted with multiple stenosis of various shapes, *Biomass Conversion and Biorefinery,* Vol. 14, pp. 1-11, 09/23, 2022.

[28] R. Ullah, R. Ellahi, S. M. Sait, S. T. Mohyud-Din, On the fractional-order model of HIV-1 infection of CD4+ T-cells under the influence of antiviral drug treatment, *Journal of Taibah University for Science,* Vol. 14, No. 1, pp. 50-59, 2020/01/01, 2020.

[29] Rahmatullah, R. Ellahi, S. T. Mohyud-Din, U. Khan, Exact traveling wave solutions of fractional order Boussinesq-like equations by applying Exp-function method, *Results in Physics,* Vol. 8, pp. 114-120, 2018/03/01/, 2018.

[30] U. Khan, R. Ellahi, R. A. Khan, S. T. Mohyud-Din, Extracting new solitary wave solutions of Benny–Luke equation and Phi-4 equation of fractional order by using (G′/G)-expansion method, *Optical and Quantum Electronics,* Vol. 49, pp. 1-14, 2017.

[31] M. M. Bhatti, R. Ellahi, S. Sait, R. Ullah, Exact solitary wave solutions of time fractional nonlinear evolution models: a hybrid analytic approach, *Bulletin of the Transilvania University of Brasov. Series III: Mathematics and Computer Science*, pp. 83-98, 09/03, 2024.

[32] A rational formulation of the equations of plastic flow for a Bingham solid, in *Proceeding of,* Cambridge University Press, pp. 100-105.

[33] J. Tripathi, B. Vasu, O. A. Bég, Computational simulations of hybrid mediated nano-hemodynamics (Ag-Au/Blood) through an irregular symmetric stenosis, *Comput Biol Med,* Vol. 130, pp. 104213, Mar, 2021. eng

[34] A. Hussain, N. Farooq, A. Ahmad, A. Saddiqa, A. S. Shflot, M. Y. Malik, Numerical Approach for Induced MHD Sutterby Fluid Flow with Electro-osmosis's function for chemical reaction and heat dissipation across the Wedge, *Case Studies in Thermal Engineering,* Vol. 56, pp. 104268, 2024/04/01/, 2024.

[35] N. Ali Shah, D. Vieru, C. Fetecau, Effects of the fractional order and magnetic field on the blood flow in cylindrical domains, *Journal of Magnetism and Magnetic Materials,* Vol. 409, pp. 10-19, 2016/07/01/, 2016.

[36] N. Nikiforakis, Computational Fluid Mechanics and Heat Transfer. By J. C. TANNEHILL, D. A. ANDERSON & R. H. PLETCHER. Taylor & Francis, 1997. 792 pp. ISBN 1 56032 045X. £58, *Journal of Fluid Mechanics,* Vol. 428, pp. 409-410, 2001.